



## Experimental and theoretical studies of surface nitrate species on Ag/Al<sub>2</sub>O<sub>3</sub> using DRIFTS and DFT

Xiuli Zhang, Hong He\*, Hongwei Gao, Yunbo Yu

Research Center for Eco-Environmental Sciences, Chinese Academy of Sciences, Beijing 100085, China

### ARTICLE INFO

#### Article history:

Received 5 February 2008

Received in revised form 27 March 2008

Accepted 22 April 2008

#### Keywords:

DFT  
DRIFTS  
TPD  
Nitrate  
Ag/Al<sub>2</sub>O<sub>3</sub>

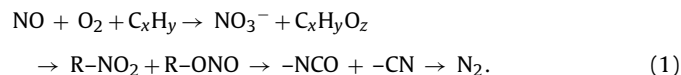
### ABSTRACT

Surface nitrate (NO<sub>3</sub><sup>-</sup>) species on the Ag/Al<sub>2</sub>O<sub>3</sub> play an important role in the selective catalytic reduction (SCR) of NO<sub>x</sub>. In this study, the formation and configuration of surface nitrate NO<sub>3</sub><sup>-</sup>(ads) species on Ag/Al<sub>2</sub>O<sub>3</sub> and Al<sub>2</sub>O<sub>3</sub> in the oxidation of NO have been studied using in situ diffuse reflectance infrared Fourier transform spectroscopy (DRIFTS) and density functional theory (DFT) calculations. Different nitrates species (bridging, bidentate and monodentate) were observed by in situ DRIFTS and validated by DFT calculations results. Attention was especially focused on the proposal of two different bidentate nitrates species (a normal bidentate and an isolated bidentate). In addition, the thermal stability of different surface nitrate species was discussed based on the adsorption energies calculations, DRIFTS, and temperature-programmed desorption (TPD) results. It was suggested that the decomposition and desorption of the surface nitrate species could be controlled by kinetics.

© 2008 Elsevier B.V. All rights reserved.

### 1. Introduction

NO<sub>x</sub> emission from the diesel and lean-burn gasoline engine caused a serious environmental problem. Since the reports in 1990 by Iwamoto et al. [1] and Held et al. [2], great effort has been devoted to the studies of active catalysts and mechanisms for the selective catalytic reduction (SCR) of NO<sub>x</sub> with hydrocarbons in excess oxygen. It is commonly accepted that Ag/Al<sub>2</sub>O<sub>3</sub> is one of the most active catalyst in the HC-SCR process [3–6]. Especially, NO<sub>x</sub> can be effectively reduced with ethanol over Ag/Al<sub>2</sub>O<sub>3</sub> even in the presence of excess O<sub>2</sub>, H<sub>2</sub>O and SO<sub>2</sub> [3,6–8]. For the elucidation of the reaction mechanism, in situ FTIR spectroscopic investigations have been applied as useful method. Several reaction mechanisms for HC-SCR have been proposed [4–6,9–11]. The common mechanism is:



The adsorbed NO<sub>3</sub><sup>-</sup> species on the Al<sub>2</sub>O<sub>3</sub> and the Ag/Al<sub>2</sub>O<sub>3</sub> play an important role in the SCR of NO<sub>x</sub>. NO<sub>3</sub><sup>-</sup> adsorbed on the Al<sub>2</sub>O<sub>3</sub> and the Ag/Al<sub>2</sub>O<sub>3</sub> materials was studied by in situ DRIFT (diffuse reflectance infrared Fourier transform) spectroscopy and TPD (temperature-programmed desorption) so far [10,12,13]. The

adsorbed NO<sub>3</sub><sup>-</sup> could be bonded to metal cations on the surface via the following adsorption structure: bridging, bidentate and monodentate (Scheme 1).

Although the surface nitrate species have been discussed and the structures were proposed in the literatures, the interpretations of the infrared spectra proposed by researchers were quite contradictory. A typical example is the band observed around 1300 cm<sup>-1</sup>, which has been attributed to monodentate nitrate [9], bidentate nitrate [10,12] or solvated nitrate [15,16], and so on. As a result, the assignment and structures of the nitrates species on Ag/Al<sub>2</sub>O<sub>3</sub> and Al<sub>2</sub>O<sub>3</sub> were still not clear.

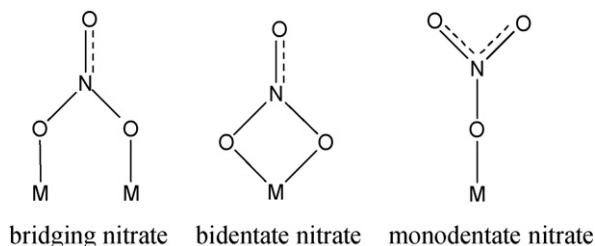
The objective of this work was to study the formation and surface structures of the nitrate species on Ag/Al<sub>2</sub>O<sub>3</sub> and Al<sub>2</sub>O<sub>3</sub> by comparing simulated IR spectra of these models calculated through density functional theory (DFT) with experimental spectra. The adsorption energy of these calculated models, associated with the in situ DRIFTS and TPD results, was also discussed.

### 2. Experimental

The Ag/Al<sub>2</sub>O<sub>3</sub> (5 wt.%) catalyst was prepared by an impregnating Al<sub>2</sub>O<sub>3</sub> (γ-type, 200 m<sup>2</sup> g<sup>-1</sup>) with an aqueous solution of silver nitrate, followed by evaporation to dryness at 393 K for 3 h and by calcinations in air at 873 K for 3 h.

In situ diffuse reflectance infrared Fourier transform spectroscopy (DRIFTS) spectra were recorded on a Nexus 670 (Thermo Nicolet) FTIR, equipped with an in situ diffuse reflection chamber

\* Corresponding author. Tel.: +86 10 62849123; fax: +86 10 62923563.  
E-mail address: [honghe@rcees.ac.cn](mailto:honghe@rcees.ac.cn) (H. He).



**Scheme 1.** Possible structures of adsorbed  $\text{NO}_3^-$  species ( $M$ =metal ion) [10,14].

and a high sensitivity MCT/A detector cooled by liquid nitrogen. The  $\text{Ag}/\text{Al}_2\text{O}_3$  catalyst for in situ DRIFTS study was finely ground and placed into a ceramic crucible. Prior to recording each DRIFTS spectrum,  $\text{Ag}/\text{Al}_2\text{O}_3$  catalyst was heated in situ in a flow of 10%  $\text{O}_2 + \text{N}_2$  at 873 K for 1 h, respectively, and then cooled to the desired temperature for taking the reference spectrum. All gas mixtures were fed at a flow rate of  $300 \text{ ml min}^{-1}$ . All spectra were measured with a resolution of  $4 \text{ cm}^{-1}$  for 100 scans.

Temperature-programmed desorption of  $\text{NO}$  ( $m/z=30$ ),  $\text{O}_2$  ( $m/z=32$ ) and  $\text{NO}_2$  ( $m/z=46$ ) was performed in a catalytic reactor. This reactor consists of a 6 mm o.d. quartz tube with a 0.5 mm o.d. thermocouple placed in the center of a bed of 20–40 mesh catalyst particles (0.2 g). A HIDEN analytical instrument, equipped with a QMS sampling system (HPR 20), was used to detect products desorbed from the catalyst. After being exposed to  $\text{NO}$  (800 ppm) +  $\text{O}_2$  (10%)/He for 60 min at 473 K, the catalyst was cooled to room temperature in He flow ( $30 \text{ ml min}^{-1}$ ), followed by heating of the sample to 973 K at a rate of  $30 \text{ K min}^{-1}$ . The MS signal of desorbed products and the temperatures were simultaneously recorded on line.

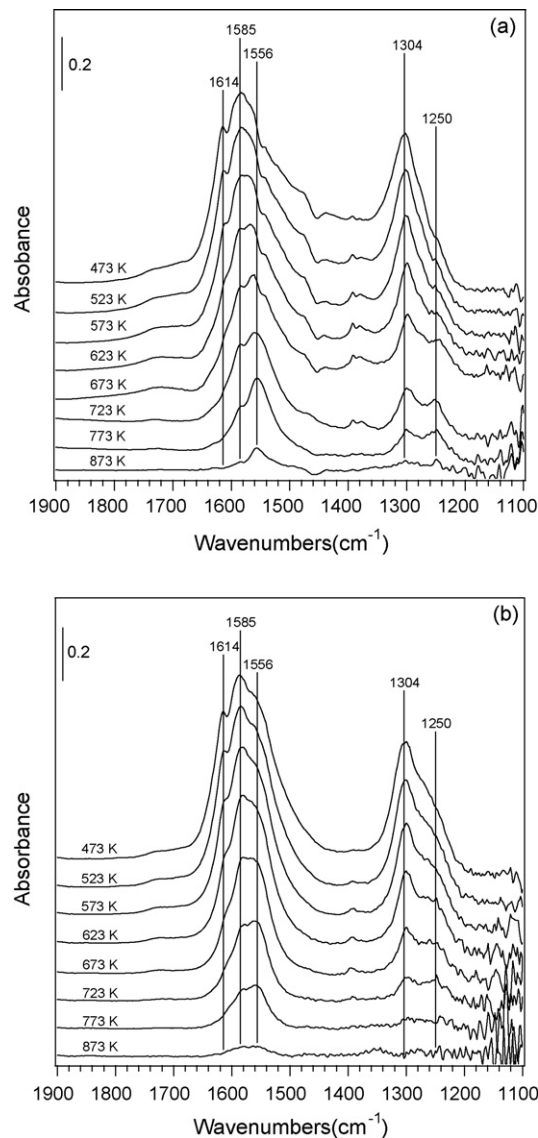
### 3. Theoretical

Density functional theory calculations were carried out by means of GAUSSIAN 98 program [17]. The properties of the calculated models were determined through the application of DFT using the B3P86 gradient corrected functional (Becke's 3 parameter function with the non-local correlation provided by the Perdew 86 expression). The LANL2DZ effective core potential basis set was used for all of the calculations. The LANL2DZ basis replaces the 1s through 2p electrons of the heavy atoms with a potential field for a considerable computational savings. A double- $\zeta$  quality Dunning basis was used for the light atoms and the remaining heavy atom electrons. Stability calculations confirmed the ground-state configuration of all the wavefunctions. The resulting vibrational frequencies and intensities were analyzed by the Hyperchem<sup>TM</sup> Version 7.0 package.

### 4. Results and discussion

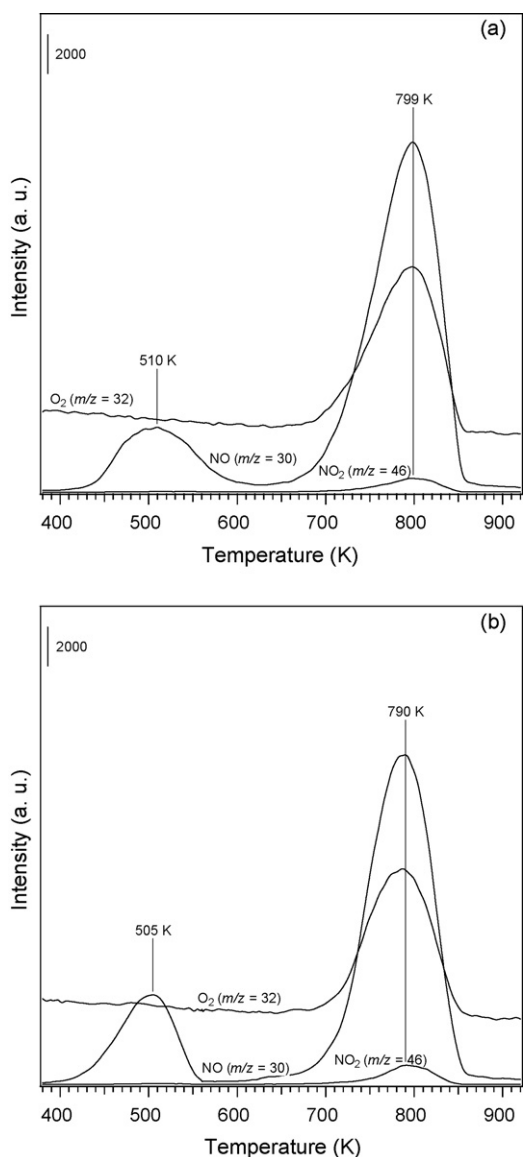
#### 4.1. Formation and thermal stability of adsorbed nitrate during $\text{NO} + \text{O}_2$ reaction over $\text{Ag}/\text{Al}_2\text{O}_3$ and $\text{Al}_2\text{O}_3$ catalysts

Fig. 1a and b show the in situ DRIFTS spectra of  $\text{Ag}/\text{Al}_2\text{O}_3$  and  $\text{Al}_2\text{O}_3$  in  $\text{NO} + \text{O}_2$  reaction at temperatures ranging from 473 to 873 K, respectively. Exposure of  $\text{Ag}/\text{Al}_2\text{O}_3$  to the fed gas at 473 K for 30 min resulted in the appearance of strong peaks at 1585, 1304  $\text{cm}^{-1}$  and shoulders at 1614, 1556 and 1250  $\text{cm}^{-1}$ , as shown in Fig. 1a. With the increase of temperature from 473 to 873 K, a significant decrease in the intensities of bands at 1614, 1585 and 1304  $\text{cm}^{-1}$  was observed, accompanied by the slow intensity decrease of the bands at 1556 and 1250  $\text{cm}^{-1}$ . At 873 K, only the



**Fig. 1.** In situ DRIFTS spectra of  $\text{Ag}/\text{Al}_2\text{O}_3$  (a) and  $\text{Al}_2\text{O}_3$  (b) at various temperatures in a flow of  $\text{NO}$  (800 ppm) +  $\text{O}_2$  (10%) +  $\text{N}_2$ .

bands at 1556 and 1250  $\text{cm}^{-1}$  were visible. In addition, a weak band at 1720–1760  $\text{cm}^{-1}$  was observed at 473 K–673 K. Decrease in IR intensity with increasing temperature is indicative of desorption/decomposition of adsorbates on  $\text{Ag}/\text{Al}_2\text{O}_3$ . Similar experiment was carried out on the surface of  $\text{Al}_2\text{O}_3$ , as shown in Fig. 1b. No obvious difference was observed between  $\text{Ag}/\text{Al}_2\text{O}_3$  and  $\text{Al}_2\text{O}_3$ , indicating that the reaction of  $\text{NO} + \text{O}_2$  occurred mainly on  $\text{Al}_2\text{O}_3$  support. This is in agreement with Miyadera's result [10]. Several vibrational spectroscopy studies of  $\text{NO} + \text{O}_2$  reaction on alumina-based material have been reported that different nitrates were formed on  $\text{Al}_2\text{O}_3$  [9,10,12,16,18]. However, the detailed assignments were inconsistent in the previous studies, especially for the band observed around 1300  $\text{cm}^{-1}$ . In this study (Fig. 1), these peaks are tentatively assigned to adsorbed  $\text{N}_2\text{O}_4$  (1720–1760  $\text{cm}^{-1}$ ), monodentate (1556 and 1250  $\text{cm}^{-1}$ ), bidentate (1585  $\text{cm}^{-1}$ ), and bridging (1614  $\text{cm}^{-1}$ ) nitrates, respectively [10,12,14]. As discussed above, the assignment of the band at 1304  $\text{cm}^{-1}$  was not clear, and it was provisionally attributed to bidentate nitrate [10,12]. The following computational section will discuss the assignments of different nitrates in more detail.



**Fig. 2.** TPD spectra of adsorbed species on Ag/Al<sub>2</sub>O<sub>3</sub> (a) and Al<sub>2</sub>O<sub>3</sub> (b) after exposure to 800 ppm NO + 10% O<sub>2</sub>/He for 60 min at 473 K.

TPD experiment was carried out for further investigation on the thermal stability of the nitrates on Ag/Al<sub>2</sub>O<sub>3</sub> and Al<sub>2</sub>O<sub>3</sub>, as shown in Fig. 2. TPD spectra of Ag/Al<sub>2</sub>O<sub>3</sub> after exposing Ag/Al<sub>2</sub>O<sub>3</sub> to NO + O<sub>2</sub> at 473 K for 60 min are shown in Fig. 2a. The observed gas-phase products were NO ( $m/z=30$ ), O<sub>2</sub> ( $m/z=32$ ) and NO<sub>2</sub> ( $m/z=46$ ). The desorption peaks of NO ( $m/z=30$ ) centered at 510 and 799 K, respectively. Compared with the desorption of NO at 510 K, the desorption of NO at 799 K was more evident and accompanied by a large amount of O<sub>2</sub> ( $m/z=32$ ) and little amount of NO<sub>2</sub> ( $m/z=46$ ). Similar result was reported by Kameoka et al. that these desorption peaks were related to the decomposition of different surface nitrate species [10]. The NO desorption at 510 K was probably originated from the decomposition of the bridging or bidentate nitrate, while the desorption of NO, O<sub>2</sub> and NO<sub>2</sub> around 799 K was due to the decomposition of the monodentate nitrates [10]. In addition, TPD spectra of Al<sub>2</sub>O<sub>3</sub> after exposing Al<sub>2</sub>O<sub>3</sub> to NO + O<sub>2</sub> at 473 K for 60 min are shown in Fig. 2b. Compared with Fig. 2a and b, no major difference between Ag/Al<sub>2</sub>O<sub>3</sub> and Al<sub>2</sub>O<sub>3</sub> was observed in the TPD measurement, indicating that the adsorption of NO + O<sub>2</sub> occurred mainly on Al<sub>2</sub>O<sub>3</sub> support.

#### 4.2. Theoretical spectra for the adsorbed nitrate species on Al<sub>2</sub>O<sub>3</sub> surface

To confirm the assignments and elucidate the vibration modes of different nitrates, DFT calculation was performed by simulating different nitrates. It has been shown that nitrate species were mostly formed on Al<sub>2</sub>O<sub>3</sub>, therefore, we designed different models for adsorbed nitrates (bridging nitrate, bidentate nitrate, free nitrate and monodentate nitrate) on Al<sub>2</sub>O<sub>3</sub> to obtain a better analysis of the nature of the nitrate species and to clarify the assignment. The optimized structures and bond lengths of the calculated models are plotted in Fig. 3. Calculated vibration frequencies, IR intensity and corresponding frequencies in the experimental spectra are listed in Table 1. Simulation spectra are presented in Fig. 4. Considering that the vibration frequencies of adsorbates can be strongly influenced by neighbor centers, we have calculated all models as far as we could image in this work, including some large cluster models. As can be seen in Figs. 3 and 4 and Table 1, the calculated results of simple models were in good agreement with experimental values, which was reasonable according to our previous studies [19–21].

Model a (see Fig. 3) was to simulate the structure of bridging NO<sub>3</sub><sup>-</sup> adsorbed on the surface of Al<sub>2</sub>O<sub>3</sub> surface. In this case, the vibration mode  $\nu(\text{N}=\text{O})$  of the bridging nitrate surface species for model a was calculated at 1607 cm<sup>-1</sup> with strong intensity 646 km mol<sup>-1</sup> (Fig. 4a), which is 7 cm<sup>-1</sup> lower than the experimental value of 1614 cm<sup>-1</sup> (Fig. 1). The calculated value is very close to the experimental values of bridging nitrate in this and the other studies [10,22].

Model b (Fig. 3) was the simulation of the bidentate adsorption of NO<sub>3</sub><sup>-</sup> on the surface of Al<sub>2</sub>O<sub>3</sub>. The vibration mode  $\nu(\text{N}=\text{O})$  of the bidentate NO<sub>3</sub><sup>-</sup> surface species for model b was calculated at 1591 cm<sup>-1</sup> with 361 km mol<sup>-1</sup> intensity (Fig. 4b), which is 6 cm<sup>-1</sup> higher than the experimental value of 1585 cm<sup>-1</sup> with strong intensity in the DRIFTS spectra (Fig. 1). However, the calculated  $\nu_{\text{as}}(\text{ONO})$  of 1170 cm<sup>-1</sup> in model b was not observed in Fig. 1. This is likely due to the strong absorption of skeletal vibration of Al<sub>2</sub>O<sub>3</sub> for frequencies below 1200 cm<sup>-1</sup>. Since the spectrum of Al<sub>2</sub>O<sub>3</sub> has been deducted as a background, the ratio of signal-to-noise was not good enough for conducting intensity analysis.

The strong band at 1304 cm<sup>-1</sup> in Fig. 1, was assigned to  $\nu_{\text{as}}(\text{ONO})$  of nitrates in previous study [18], whereas, no adsorption feature in Fig. 4b could be related with the strong band at 1304 cm<sup>-1</sup>. Therefore, we proposed that the band at 1304 cm<sup>-1</sup> could originate from other vibrational structures and calculated all models as far as we could image. Up to now, only model c is reasonable to account for the nature of band at 1304 cm<sup>-1</sup> as shown in Fig. 3. Fig. 4c shows that the computed IR vibration frequency for model c was 1322 cm<sup>-1</sup>, which is close to the experimental data of 1304 cm<sup>-1</sup> (Fig. 1). Model c configuration of nitrate adsorbed on bare Al atom indicates that lattice oxygen was involved in the formation of surface nitrate [23]. In addition, the vibration mode in the simulated spectrum in Fig. 4c was attributed to the N=O stretch vibration, rather than the  $\nu_{\text{as}}(\text{ONO})$  vibration [18]. On the basis of the above results, the calculated model c provided an actual structure to understand and clarify the assignment of the band at around 1300 cm<sup>-1</sup>. Compared with Fig. 3b and c, two kinds of bidentate nitrates located in the different chemical environment, which resulted in the difference of calculated spectra in Fig. 4b and c. Accordingly, we defined models b and c as a normal bidentate nitrate and an isolated bidentate nitrate, respectively.

Grassian and coworkers [15,16] proposed that the adsorption peak of the free solvated nitrate aqueous ion over Al<sub>2</sub>O<sub>3</sub> at 298 K was also around 1302 cm<sup>-1</sup> and the addition of water promoted the formation of free nitrate. Accordingly, we calculated the

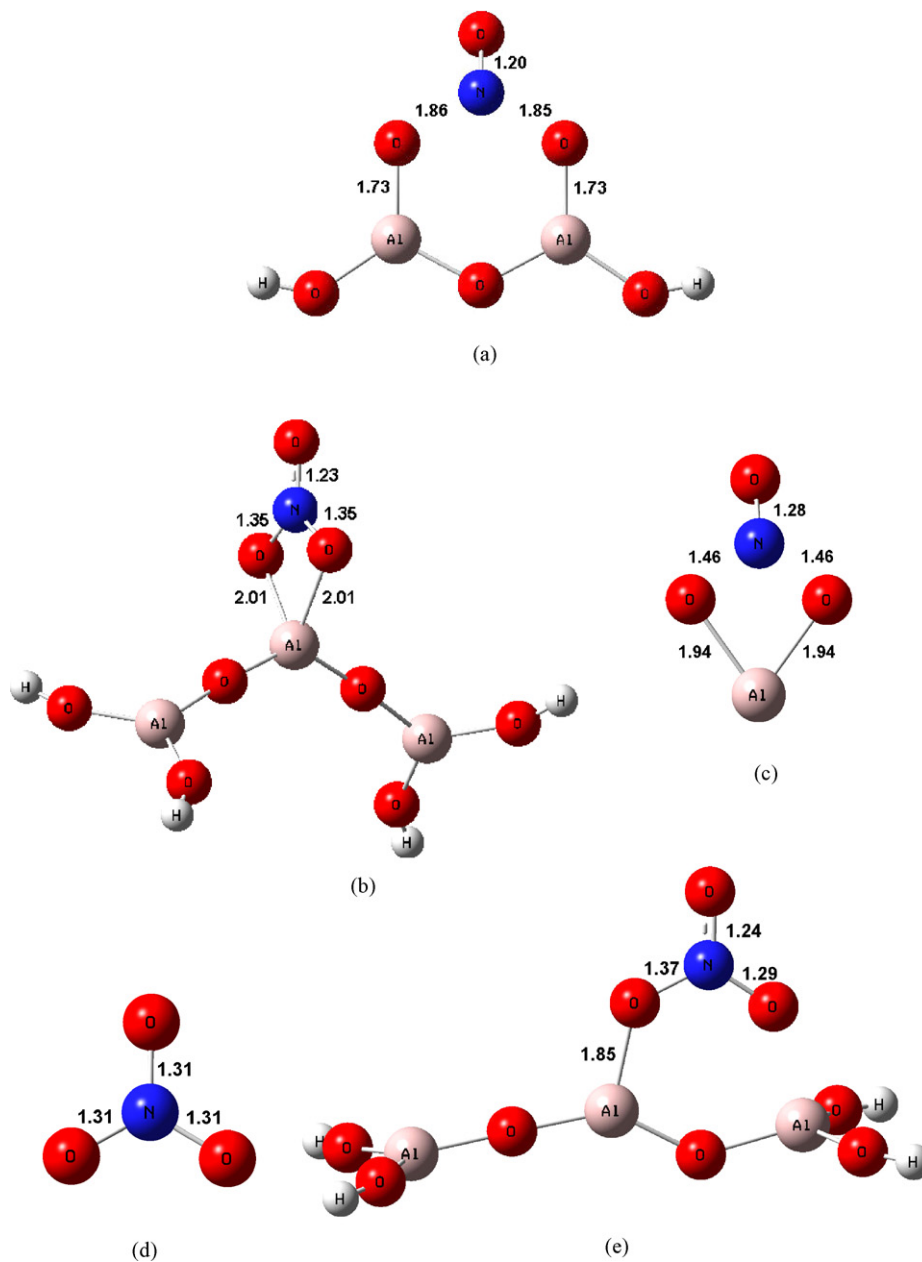


**Fig. 3.** Optimized configuration and bond distances of calculation models for nitrates on  $\text{Al}_2\text{O}_3$  (a–c and e) and uncoordinated nitrate ion (d).

**Table 1**

Calculated vibration frequencies and IR intensity for the six calculated models at the B3P86/LANL2DZ level and corresponding frequencies in the experimental spectra

Surface species	Model	Frequency ( $\text{cm}^{-1}$ )	Intensity ( $\text{km mol}^{-1}$ )	Experiment ( $\text{cm}^{-1}$ )	Vibration mode
Bridging nitrate	a	1607	646	1614	$\nu(\text{N}=\text{O})$
Normal bidentate nitrate	b	1591	361	1585	$\nu(\text{N}=\text{O})$
		1170	305	–	$\nu_{\text{as}}(\text{ONO})$
Isolated bidentate nitrate	c	1322	270	1304	$\nu(\text{N}=\text{O})$
Uncoordinated nitrate	d	1327	408	–	$\nu_{\text{as}}(\text{ONO})$
		1324	409	–	$\nu(\text{N}=\text{O})$
Monodentate nitrate	e	1530	397	1556	$\nu(\text{N}=\text{O})$
		1212	415	1250	$\nu_{\text{as}}(\text{ONO})$

(–) Not observed.

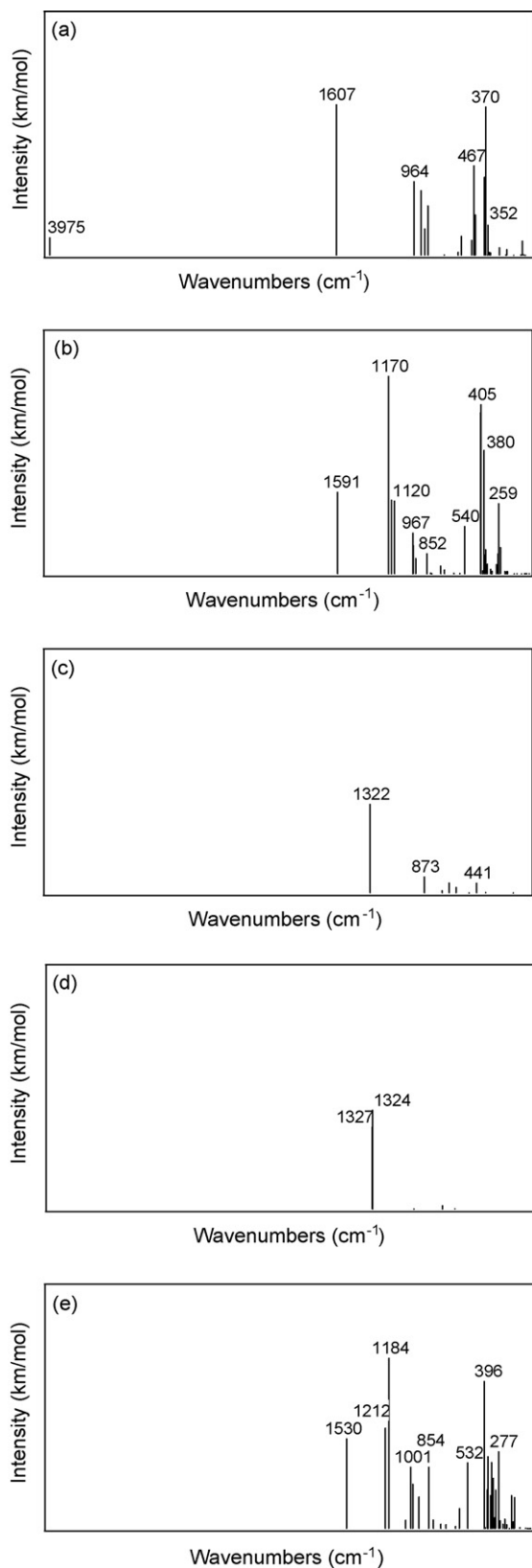


Fig. 4. Calculated IR spectra for the computational models (a–e) of surface nitrate species on  $\text{Al}_2\text{O}_3$  at B3P86/LANL2DZ level.

uncoordinated nitrate ions as shown in model d (Fig. 3), and the simulated IR spectrum and frequency were shown in Fig. 4d and Table 1, respectively. The calculated result  $1327\text{ cm}^{-1}$  with  $\nu_{\text{as}}(\text{ONO})$  vibration mode and  $1324\text{ cm}^{-1}$  with  $\nu(\text{N}=\text{O})$  vibration mode of model d were adjacent to the experimental value  $1304\text{ cm}^{-1}$ . The N–O average distance was  $1.31\text{ \AA}$ . It seems that the model d was reasonable to account for the assignment of the band at  $1304\text{ cm}^{-1}$ . However, it must be mentioned that the removal of the adsorbed water on heated and dehydrated  $\text{Al}_2\text{O}_3$  could eliminate the solvated nitrate aqueous ion and form the oxide-coordinated nitrate around  $1302\text{ cm}^{-1}$  [15]. Therefore, the model d for the water-solvated nitrate was not fit for our experimental condition because the gas mixture was dry and the catalyst was pretreated at  $873\text{ K}$  for  $60\text{ min}$  before collecting the spectra.

As for the calculated models for monodentate absorption of  $\text{NO}_3^-$  on  $\text{Al}_2\text{O}_3$ , model e (Fig. 3) was adopted for the simulation of vibration frequency. The calculated  $\nu(\text{N}=\text{O})$  and  $\nu_{\text{as}}(\text{ONO})$  vibration frequencies of this monodentate  $\text{NO}_3^-$  surface species were  $1530\text{ cm}^{-1}$  with  $397\text{ km mol}^{-1}$  intensity and  $1212\text{ cm}^{-1}$  with  $415\text{ km mol}^{-1}$  intensity, respectively (Fig. 4e). The computed frequencies of model e are very close to the experimental values ( $1556$  and  $1250\text{ cm}^{-1}$ ). The assignment of the calculated  $\nu(\text{N}=\text{O})$  and  $\nu_{\text{as}}(\text{ONO})$  vibration modes is in agreement with the literature [12,22].

#### 4.3. Adsorption energy of surface nitrate on $\text{Al}_2\text{O}_3$

The in situ DRIFTS results obviously demonstrate that the different nitrates adsorbed on the  $\text{Al}_2\text{O}_3$  surface had different thermal stabilities. To further obtain insights into the thermal stabilities of different nitrates, we compared the adsorption energies of the calculated models ((a) bridging; (b) normal bidentate; (c) isolated bidentate; (e) monodentate nitrate) in Fig. 3. Here, adsorption energy ( $E_{\text{ads}}$ ) was defined by the following equation:

$$E_{\text{ads}} = E_{\text{cluster/adsorbate}} - E_{\text{cluster}} - E_{\text{adsorbate}} \quad (2)$$

where  $E_{\text{cluster/adsorbate}}$  is the total energy of the adsorbate on the cluster,  $E_{\text{cluster}}$  is the total energy of the bare cluster (aluminium), and  $E_{\text{adsorbate}}$  is the energy of the gas-phase adsorbate.

The calculated  $E_{\text{ads}}$  of models a, b, c and e are  $-75.89$ ,  $-62.53$ ,  $-52.92$  and  $-58.58\text{ kcal mol}^{-1}$ , respectively. The negative  $E_{\text{ads}}$  values indicate that the adsorbed state (cluster/adsorbate) is energetically favorable. The difference in adsorption energy among the model a, b, c and e is attributed to structural difference. The results show that the order of stability in the nitrates species adsorbed on the  $\text{Al}_2\text{O}_3$  catalyst is a (bridging) > b (normal bidentate) > e (monodentate) > c (isolated bidentate) in the view of thermodynamics. In contrast, the order of thermal stability of nitrates species adsorbed on  $\text{Al}_2\text{O}_3$  was monodentate > bidentate or bridging, which was confirmed by DRIFTS (Fig. 1b). As a result, we conjectured that the decomposition and desorption of different nitrates was controlled by kinetics.

## 5. Conclusions

On the basis of the in situ DRIFTS study, we found that various (bridging, bidentate and monodentate) nitrate species were formed on  $\text{Ag}/\text{Al}_2\text{O}_3$  by the reaction between  $\text{NO}$  and  $\text{O}_2$ . The vibrational modes of nitrate species were simulated and analyzed by Gaussian 98 and hyperchem 7.0 program. Based on the density functional theory calculations, the models a, b and e were established to describe the exact structures of the bridging ( $1614\text{ cm}^{-1}$ ), bidentate ( $1585\text{ cm}^{-1}$ ) and monodentate ( $1556$  and  $1250\text{ cm}^{-1}$ ) nitrates species on  $\text{Al}_2\text{O}_3$ , respectively. Noticeably, the band at  $1304\text{ cm}^{-1}$

is assigned to an isolated bidentate nitrates species, whose formation could involve lattice oxygen of  $\text{Al}_2\text{O}_3$ . For the thermal stability of different nitrates on  $\text{Al}_2\text{O}_3$ , the calculated order of adsorption energy was not identical with the experimental order of thermal stability. Accordingly, the decomposition and desorption of nitrate species are probably controlled by kinetics.

### Acknowledgments

This work was financially supported by the National Natural Science Foundation of China (20425722) and the Knowledge Innovation Program of the Chinese Academy of Sciences (RCEES-QN-200710) and the Special Funds for Young Scholars of RCEES, CAS.

### References

- [1] M. Iwamoto, H. Yahiro, S. Shundo, Y. Yu-u, N. Mizuno, *Appl. Catal.* 69 (1991) L15.
- [2] W. Held, A. König, T. Richter, L. Pupper, SAE Paper, 1990, 900496.
- [3] T. Miyadera, *Appl. Catal. B* 2 (1993) 199.
- [4] R. Burch, J.P. Breen, F.C. Meunier, *Appl. Catal. B* 39 (2002) 283.
- [5] A. Satsuma, K. Shimizu, *Prog. Energy Combust. Sci.* 29 (2003) 71.
- [6] H. He, Y.B. Yu, *Catal. Today* 100 (2005) 37.
- [7] S. Sumiya, M. Saito, H. He, Q.C. Feng, N. Takezawa, *Catal. Lett.* 50 (1998) 87.
- [8] A. Abe, N. Aoyama, S. Sumiya, N. Kakuta, K. Yoshida, *Catal. Lett.* 51 (1998) 5.
- [9] K. Shimizu, J. Shibata, A. Satsuma, T. Hattori, *Phys. Chem. Chem. Phys.* 3 (2001) 880.
- [10] S. Kameoka, Y. Ukisu, T. Miyadera, *Phys. Chem. Chem. Phys.* 2 (2000) 367.
- [11] Y.B. Yu, H. He, Q.C. Feng, H.W. Gao, X. Yang, *Appl. Catal. B* 49 (2004) 159.
- [12] F.C. Meunier, J.P. Breen, V. Zuzaniuk, M. Olsson, J.R.H. Ross, *J. Catal.* 187 (1999) 493.
- [13] K. Shimizu, H. Kawabata, A. Satsuma, T. Hattori, *J. Phys. Chem. B* 103 (1999) 5240.
- [14] K.I. Hadjiivanov, *Catal. Rev. Sci. Eng.* 42 (2000) 71.
- [15] T.M. Miller, V.H. Grassian, *Geophys. Res. Lett.* 25 (1998) 3835.
- [16] G.M. Underwood, T.M. Miller, V.H. Grassian, *J. Phys. Chem. A* 103 (1999) 6184.
- [17] M. Frisch, J. Foresman, A. Frisch, et al., *Gaussian 98*, Gaussian Inc., Pittsburgh, PA, 1998.
- [18] W.S. Kijlstra, D.S. Brands, E.K. Poels, A. Bliet, *J. Catal.* 171 (1997) 208.
- [19] H.W. Gao, H. He, *Spectrochim. Acta A* 61 (2005) 1233.
- [20] H.W. Gao, H. He, Y.B. Yu, Q.C. Feng, *J. Phys. Chem. B* 109 (2005) 13291.
- [21] Q. Wu, H.W. Gao, H. He, *J. Phys. Chem. B* 110 (2006) 8320.
- [22] T.J. Toops, D.B. Smith, W.S. Epling, J.E. Parks, W.P. Partridge, *Appl. Catal. B* 58 (2005) 255.
- [23] Y. Chi, S.S.C. Chuang, *J. Phys. Chem. B* 104 (2000) 4673.